

TECHNICAL MEMORANDUMS

NATIONAL ADVISORY COMMITTEE FOR AERONAUTICS

No. 992

STATISTICAL ANALYSIS OF THE TIME AND FATIGUE
STRENGTH OF AIRCRAFT WING STRUCTURES

By Hans W. Kaul

Jahrbuch 1938 der Deutschen Luftfahrtforschung

Washington
October 1941



NATIONAL ADVISORY COMMITTEE FOR AERONAUTICS

TECHNICAL MEMORANDUM NO. 992

STATISTICAL ANALYSIS OF THE TIME AND FATIGUE
STRENGTH OF AIRCRAFT WING STRUCTURES*

By Hans W. Kaul

SUMMARY

The results from stress measurements in flight operation afford data for analyzing the frequency of appearance of certain parts of the static breaking strength during a specified number of operating hours. Appropriate frequency evaluations furnish data for the prediction of the required strength under repeated stress in the wing structures of aircraft of the different stress categories for the specified number of operating hours demanded during the life of a component. The measures adopted obviously will depend on the magnitude and frequency of the loads during the life of the aircraft and will vary with the type of aircraft, purpose of use, and atmospheric conditions (gustiness).

The author has subjected to statistical analysis a large number of data covering the wing stressing of six different civil aircraft ranging in weight from 2000 to 6000 kilograms. At the same time the stress frequency of application curves for three acrobatic aircraft is investigated. Thus, it is possible to estimate the probable number of times loads of a given magnitude will be applied to the wing structure over flying time ranging from 2000 to 6000 hours, (life of aircraft depending on class), and to adjust the ground tests accordingly.

I. INTRODUCTION

Heretofore, aircraft structures were designed to fulfill certain static strength requirements, and the strength

*"Die erforderliche Zeit- und Dauerfestigkeit von Flugzeugtragwerken." Jahrbuch 1938 der deutschen Luftfahrtforschung, pp. I 274-I 288.

specifications of the leading aeronautical countries showed general agreement. It is true that certain parts, such as wing roots and control surfaces, were designed to take into account fatigue limits, but this factor was not applied to the wing structure as a whole. As a result there is still considerable confusion regarding the necessary strength of the separate structural groups of an airplane under frequent load reversals. The present report is intended to bridge this gap as far as the wing structure is concerned. The comparatively high service stresses in wing structures of modern high-speed aircraft and the increasing hours of operation during the life of the individual parts make the study of the required time strength and fatigue strength for this group appear particularly urgent. The scope of the time strength includes the stresses which the wing can withstand more than once but not indefinitely, hence is situated between the static breaking strength and the fatigue strength, but does not include these two extreme values.

Investigations of this kind must, as a rule, be carried out separately for the two principal stress groups, namely, the stresses due to operation of the controls by the pilot, and those due to atmospheric conditions (gustiness).

Studies of gust stresses must, in turn, be grouped in the determination of the form of distribution curves of the operating stresses at different gust intensities and in the determination of the frequency of appearance of a gust of certain intensity in yearly average. The latter must be made for a specific climatic zone in relation to the flying height.

II. DETERMINATION AND REPRESENTATION OF THE DISTRIBUTION CURVES OF OPERATING STRESSES

A. Choice of Characteristic Quantity

for Wing Structure Stress

As indication of the stress, either the accelerations at right angles to the plane of the wing in the airplane center of gravity, or the deflections of the wing of the

strains of highly stressed wing components, such as the beam flanges, may be chosen. Under the conditions of high wing stresses it involves, in the greater majority of cases, flight conditions, that is, angle-of-attack ranges, within which modern airfoils manifest only little center-of-pressure travel, so that the three cited test quantities for the wing stress are proportional to each other. By reason of this fact none of the three possibilities merits, for the present, any preference over the other. The exception is the very "hard" stress, for example, by elevator operation with very great control speed or in gusts where the gust velocity along the airplane rises very rapidly. Then it may happen that the wing swings beyond the equilibrium position corresponding to the applied air force. (See reference 2, sec. VI.) In this case, then, the wing would be subject to higher stresses than the test value for the acceleration in the center of gravity would predict. In this instance the measurement of strains or deflections would merit preference over the accelerations. However, since acceleration recording is the simplest method from the point of view of measurement as well as of evaluation, some comparative tests by the DVL included both acceleration as well as strain and deflection measurements.

Figures 1(a) and 1(b) show the result of such measurements on the Albatros L 83 airplane, which, with its comparatively great aspect ratio and low natural wing bending frequency (3.5 Hz) appeared particularly suited for studies of this kind. Figure 1(a) shows the accelerations computed from the deflection measurement, figure 16, those computed from the strain measurement for a large number of separate test points plotted against the concurrently measured center-of-gravity acceleration. The result indicates that the individual points fill almost evenly a scattering zone corresponding to the instrumental and evaluating accuracy, and that measurable systematic departures in the previously cited direction are absent. Accordingly, it appears justified for the present to stay with acceleration measurements. This, of course, necessitates an occasional check if the ratio of flying speed to natural wing bending frequency evinces a substantial increase during the development. On the Albatros L 83 this

ratio amounts to $\frac{v h}{v} = \frac{50}{3.5} \approx 14 \text{ m/s}$, or $\frac{v h}{v t_m} = \frac{50}{3.5 \times 2.4} \approx 6^*$

*Subsequent evaluation of tests by Küssner and Taub on Junkers F 13 and BFW M 20b2, which possess lower ratios $\frac{v h}{v} t_m$ than the Albatros L 83, afforded the same results as given above.

the speed being expressed in multiples of chord per second.

For completion a further difference between acceleration measurements on the one hand and deflection or strain measurements on the other is pointed out:

While, as a rule, the acceleration following a single gust either dies down aperiodically, after exceeding the maximum value to the value lg corresponding to unaccelerated level flight, or else drops slightly below lg (cf. fig. 1(c)), the wing usually executes several strongly damped vibrations during the damping out of the stress. In section III it will be shown that this difference also is of no significance for the present study.

B. Type of Frequency Appraisal

The frequency of appearance of certain stresses within the measuring period can be expressed in various forms. Essentially three possibilities are involved:

- a) "Frequencies of the first kind" (H_1) indicate the number of maximums or minimums of the function $Y = f(t)$ - that is, test value Y of the stress with respect to time - during the total measuring period T each between two extreme values Y_i and Y_{i+1} , the maximums being counted by stresses Y_i , which, by equal prefix are greater in amount than stress Y_{stat} corresponding to unaccelerated level flight, hence maximum in the case of $Y_i \geq Y_{stat}$, and minimum in the case of $Y_i \leq Y_{stat}$;
- b) "Frequencies of the second kind" (\bar{H}_1) indicate the number of times that a certain threshold value Y_i of the curve $Y = f(t)$ is passed in ascending direction in the $Y_i \geq Y_{stat}$ range and in descending direction in the $Y_i \leq Y_{stat}$ range;
- c) "Frequencies of the third kind" (H_1) indicate the number of times that a certain threshold value Y_i of the function $Y = f(t)$ is passed in ascending and descending direction.

The frequencies of the first and second types can be calculated with sufficient accuracy from those of the third type and vice versa. The selection should therefore be made chiefly with respect to the evaluation technique and so is governed by the chosen recording process, the quality of the records and the evaluating means involved, such as automatic counters. In the present article the type of frequencies in the individual cases is given. All data are reduced to frequencies of the first type as the most suitable.

C. Selection of Class Division for Evaluation

The class division ΔY , that is, the distance between two adjacent threshold values Y_i and Y_{i+1} , employed in the evaluation is chosen constant over the total range of statistics and small enough to be consistent with the accuracy expected by the employed method of evaluation. The class intervals as much as possible are so located that the stress Y_{stat} in unaccelerated level flight forms the boundary of one class.

The amount of ΔY for investigations of wing stresses is ordinarily chosen so as to correspond to a change of $\Delta n \approx 0.2$ to 0.3 in the load factor, since the selection of smaller values Δn does not enter into question by the existent evaluation accuracy. This classification is, at the same time, small enough to make a minor change in the choice of amount of ΔY of little effect on the average values and spread bands of the measured distributions, and still enable the prediction of the frequencies of the first type from recorded frequencies of the second type, etc., with adequate accuracy.

D. Average Values and Spread Bands

of Measured Distributions

Measured stress distributions are represented for the time being by tables or polygons of distribution (for example, see table I and fig. 2). For comparing different distributions by stating one or more characteristic values, averages and spread bands are resorted to.

The most commonly used average values are:

1. The arithmetical mean:.

$$M = \frac{\sum H_i Y_i}{\sum H_i} \quad \left. \begin{array}{l} (Y_i \text{ argument value}) \\ H_i \text{ frequency} \end{array} \right\} \text{ of class } i)$$

$$\sum H_i = N \quad \text{extent of statistics;}$$

2. The central value C that divides the extent of the arranged statistics in two equal parts, that is, as many observations above as below it;
3. The densest value D , that is, the area of maximum frequency H_{\max} .

TABLE I

Flight with D 2026, BFW M 20 b₂ (Marseille to Montélimar and back), February 22, 1932 (evaluated 86.8 minutes in the 31st to the 128th minute of flight).

[$\Delta y = 20$ mm; corresponding load factor $\Delta n = 0.155$]

i	Y_i^* (mm)	H_i	Load factor $n_{Y_i} = \frac{Y_i}{Y_{\text{stat}}}$
1	41	1	0.318
2	61	16	.473
3	81	139	.628
4	101	651	.783
5	121	1432	.938
6	141	1248	1.093
7	161	259	1.248
8	181	53	1.403
9	201	4	1.558

* Y_i wing deflection referred to stressless state.

By the determination of average values for recorded wing stress distributions, it was found that the three averages M , C , and D differed by such small amounts that the differences are within the evaluation accuracy and that the amount $M = C = D$ practically coincides with the stress Y_{stat} for unaccelerated level flight. It therefore appears expedient when comparing measured distribution polygons to plot the separate graphs above one another so that the readily ascertainable arithmetical mean M of the individual distributions becomes congruent. This applies in particular to measured distributions of strains and deflections where the amount of Y_{stat} frequently does not lend itself to a sufficiently exact determination beforehand. (In distributions of accelerations Y_{stat} is, of course, equal to $1g$.)

The most commonly used spread bands are:

1. The average departure δ , that is, the arithmetical mean of the absolute values of the departure $\delta_i = |Y_i - MW_i|$ from a certain average MW ;
2. The mean departure $\mu = \sqrt{\frac{1}{N} \sum H_i \delta_i^2}$;
3. The variation width $B = \frac{Y_{max} - Y_{min}}{MW}$;
4. The slope $Sch = \frac{M - D}{\mu}$ (measure for the asymmetry).

The described results respecting the averages make it immediately apparent that the slope Sch as indication for an asymmetry of the wing stress distributions is not practical relative to its average value M . In such cases it is common practice to define δ or μ and B for each part on either side of M separately and to express the asymmetry by the difference δ' and δ , or μ' and μ or B' and B , upwardly and downwardly.

Of the departures δ and μ the mean μ has proved superior as characteristic value for distributions to the average δ . This centers the problem of characteristic quantities for distributions of the type in question chiefly in the mean departure:

$$\mu = \sqrt{\frac{\sum H_i \delta_i^2}{N}} \quad \delta_i = |Y_i - MW| \quad (1)$$

and the related upward and downward departures

$$\mu' = + \sqrt{\frac{\sum H_i \delta_i'^2}{N'}} \quad \begin{aligned} \delta_i' &= |Y_i' - MW| \\ Y_i' &\geq MW \end{aligned} \quad (1a)$$

$$\mu_1 = - \sqrt{\frac{\sum H_i \delta_i^2}{N}} \quad \begin{aligned} \delta_i_1 &= |Y_i_1 - MW| \\ Y_i_1 &\leq MW \end{aligned} \quad (1b)$$

and in the variation width

$$B = \frac{Y_{\max} - Y_{\min}}{M} \quad (2)$$

and the related upward and downward

$$B' = \frac{Y_{\max} - M}{M} \quad (2a)$$

$$B_1 = \frac{Y_{\min} - M}{M} \quad (2b)$$

E. Distribution Functions

The most accurate description of a given distribution is afforded by a distribution function. Such functions permit, moreover, an extrapolation, for instance, to expected variation widths under longer operating periods than the measuring period amounted to.

The best known functions employed for describing measured distributions are variations of Gauss' normal distribution. But their applicability is contingent upon the distributions possessing the distinctive mark of irregularity; thus, they are generally unsuitable for reproducing distributions recorded over long flight distances under different weather conditions and contour of terrain. In

one instance (stresses on the control surfaces of the Graf Zeppelin during protracted service period) the description of the frequency curves was enabled through the following distribution function of the named type:

$$H_1 = c e^{-b^2(Y-a)^2}$$

Küssner (reference 3) had been able to use a special form of this function, namely,

$$H_1 = \frac{\Delta Y \bar{C}}{\mu \sqrt{\pi}} e^{-t^2}$$

with

$$t = \frac{Y - Y_{stat}}{\mu} + \beta$$

for describing several wing-stress distributions, at whose determination a selection from the total number of test values had been artificially effected in such a way that the assumptions for applying a Gauss type distribution function had been complied with. He also quotes numerical values for the constants $\bar{C} = \log \bar{C}$ and β for the particular selective distributions.

Ordinarily it is merely possible to describe certain wing-stress distributions by sufficiently many terms of a suitable series, such as the Bruns φ series, which proceeds along differential quotients of Gauss' normal distribution. Such a representation entails, of course, considerable paper work, especially if a certain "quality of adaptation" is specified. Such procedure is necessary if on the basis of considerations of the failure expectancy time (reference 3) the necessary static strength, that is, the breaking strength for one-time load is to be determined, but which may be dispensed with for the purposes in question.

III. DISTRIBUTION CURVES OF OPERATING STRESSES OF AIRCRAFT WING STRUCTURES IN FLIGHT IN GUSTS

A. Comparison of Statistical Data on Different Aircraft Types

In order to compare statistical data of stresses in flight operation secured on different types of aircraft or under dissimilar operating conditions, a uniform, non-dimensional reference quantity is employed for the stresses. The component of the acceleration at right angles to the plane of the wing in the airplane center of gravity serves as absolute criterion for stress in the wing structure.

A comparison of test values for gust accelerations secured on different types of aircraft or at different flying speeds requires a reference value which permits the exclusion of the influence of the design quantities, of the aircraft characteristics, and that of the flying speed, so that the effect of gusts can be analyzed by itself.

Such a reference value that meets the cited requirements rigorously is, at the present state of research, impossible. But it can be shown that the safe load factor specified in the requirements for the load case "stress of wing structure due to gust" (BVF, fig. 1142, case 115)

$$n_{G_{safe}} = 1 + q \frac{F_{Tr}}{G} \frac{v_b}{v} \frac{dc_{aTr}}{d\alpha} \eta \quad (3)$$

(index Tr denotes wing structure)

v_b gust velocity

η gust effect factor (Cipher 1142, of BVF)

does represent a practical comparative value. The factor $n_{G_{safe}}$ indicates the multiple of acceleration of gravity $g = 9.81 \text{ ms}^{-2}$, measured in the airplane center of gravity, when the airplane enters at speed v in a sharply defined

gust directed at right angles to the flight path, the gust having the flow velocity v_b with respect to the surrounding still air. In the analysis of the aerodynamic forces and moments during entry in the gust, it is assumed that all rotatory motions of the aircraft about its lateral axis can be disregarded.

The safe load factors $n_{G_{safe}}$ for the gust velocity $v_b = 10$ m/s specified in the strength requirements were computed according to equation (3) for seven types of aircraft for which the test data on gust accelerations over a long period of operation were available. The factor η of the gust effect was defined in conformity with cipher 1142 of the BVF as gross weight G , the amount existing at the time of the test flight, was employed. The maximum horizontal speed v_h at full throttle specified in the strength requirements was substituted by the mean speed $v_{cruising}$ available during the tests as flying speed v , since the test flights were in part carried out with different throttle settings, so that the full throttle speed v_h affords no practical measure of comparison.

In figure 3 the thus-obtained approximate values obtained during specific test periods in gust flights with different airplanes. The explored types involved very dissimilar aircraft as regards dimensions, aspect ratio, that is, the values $\frac{dca}{d\alpha}$, and design (monoplanes and biplanes) as well as flight characteristics, particularly as to static longitudinal stability; the wing loading $\frac{G}{F_{Tr}}$ ranged between 40 and 90 kg/m², the flying speeds between 140 km/h and 325 km/h during the tests. Even so, the agreement between the recorded maximum values and the $n_{G_{safe}}$ values is satisfactory; the discrepancies in the face of a scattering zone of around 0.2g anticipated on account of instrumental and mathematical inaccuracy alone, ranged within 0.4g.

Systematic departure of test values from the safe load factor $n_{G_{safe}}$ manifested itself to the extent that the maximum accelerations measured in gusty weather during a total test period of 20 hours or more are generally situated above the approximate values $n_{G_{safe}}$ computed

for a gust velocity $v_b = 10 \text{ ms}^{-1}$ and $v = v_{\text{cruis}}$; whereas the maximum values obtained within 8 hours or fewer of flight remain generally below the approximate values. This result might suggest making the "comparative gust velocity" v_b dependent on the total test period, in as much as during longer test periods the one-time occurrence of a particularly high gust velocity possesses greater probability than during a short time test. However, this refinement was disregarded, since its effect on the result of frequency studies is certainly not decisive.

The load factor n_g for a gust velocity $v_b = 10 \text{ ms}^{-1}$ conformable to the strength specifications is, at the same time, an appropriate reference value for stress analysis, since the principal components of commercial aircraft wing structures are largely measured in compliance with the requirements of the load case: "wing stress due to gust," so that gust acceleration data in fractions of n_g represent, at the same time, the data in fractions of the static breaking load of the wing structure; according to the present German Specifications (1936 ed.) the ultimate load factor $n_{g_{\text{failure}}}$ is equal to 1.8 times the safe load factor $n_{g_{\text{safe}}}$. These reasons make the factor $n_{g_{\text{safe}}}$ appear a suitable reference value for gust stress measurements. In the following, therefore, the acceleration changes due to gusts relative to the state of unaccelerated horizontal flight ($n = 1$) are given in fractions of

$$(n_{g_{\text{safe}}} - 1) = q \frac{F_{\text{Tr}}}{G} \frac{v_b}{v} \frac{dca_{\text{Tr}}}{d\alpha} n(v_b = 10 \text{ ms}^{-1}) \quad (3a)$$

In a comparison of measured frequencies H_i for a certain stress category i it should be borne in mind that the absolute frequencies H_i depend upon the total measuring period as well as upon the speed of the experimental aircraft, for a fast machine hits a greater number of gusts per unit time than a slow one. But there are still other influences on the gust frequency, that is, the number of gusts per unit time recorded in the air-plane, as will be shown later. It is therefore advisable to extend the comparison between dissimilar test series not to the absolute frequencies H_i , but rather to the

relative frequencies

$$h_i = \frac{H_i}{N} \quad (N = \sum H_i = \text{scope of statistics} = \text{total number of test values}).$$

Through the relative frequencies h_i of the separate stress categories the form of the stress distribution polygon is defined, while the scope of the statistics is defined by the mean gust frequency and the total operating and total test period, respectively.

B. Form of Distribution Polygons for Different Aircraft and Dissimilar Operating Conditions

First, it is shown that the form of the distribution polygons is comparatively little affected by the gust intensity and the explored airplane type. The gust intensity is expressed according to the Darmstadt gust scale (reference 4), which divides the degrees of gustiness into "still" and "gusty b_0 " to "gusty b_3 ." A discussion of the use of the scale together with its accuracy follows elsewhere in the report.

Figures 4 to 6 show a series of recorded gust stress distribution polygons, in which the relative frequencies h_i are plotted for the separate stress categories i . The criterion chosen for the wing structure stress is the previously cited nondimensional proportional value

$$\frac{b_i - 1}{n_{G_{\text{safe}}} - 1} \quad (b_i = \text{acceleration corresponding to the middle of class } i, \text{ measured in multiples of the acceleration of gravity } g).$$

Figure 4 contains a series of distributions obtained on the same airplane part (D - JDUH, type Heinkel He 45 D) in flights with the same flying weight and the same flying speed on days at which the airplane pilot reported gust intensity b_1 . The results of the individual flights, lasting from $\frac{1}{2}$ to 1 hour each, are scattered within certain limits throughout the distribution polygon (solid lines, fig. 4) comprising the total test period of about $3\frac{1}{2}$ hours. Figure 5 shows for the same airplane weight and speed the distributions (average values for the total measuring periods shown in the graph) recorded in gust

intensities b_0 , b_1 , b_2 , and b_3 . The shapes of the distribution polygons in both plots are seen to vary within fairly moderate limits, while the plotted amounts for the departures μ , μ' , and μ'' are all located within a short interval (between 0.09 and 0.15).

Figure 6 gives the gust stress distributions compiled on six different types of aircraft, as recorded in flight tests.

The types of aircraft comprised

TABLE II

Type	Design	Total weight at test (kg)	Wing loading (kg/m ²)	Reference
Albatros L 83	low wing monoplane	2600	43.7	ZFM 1931, pp. 380-81.
Junkers F 13		1950	45.4	Taschenbuch der Luftflotten 1927, p. 138.
Junkers G 24		5800	65.4	Taschenbuch der Luftflotten 1927, p. 140.
Heinkel He 45 D	biplane	2560	74	Handbuch der Luftfahrt 1937-38, p. 179.
Heinkel He 70	low wing monoplane	3200	87	ZFM 1933, pp. 669-76.
Junkers Ju 160		3270	94	ZVDI 1935, pp. 419-24.

In spite of the marked discrepancies regarding dimensions, flight characteristics, speeds, wing loading, and the comparatively short total measuring periods, figure 6 manifests a surprisingly good agreement of the individual distributions as to form and values μ . In fact they do not differ much from the distributions in figure 5 which refer to only one airplane type at different degrees of gustiness. Hence, it follows that in fatigue-strength

studies a "unit distribution" could be used as basis for the form of the relative frequency distribution curve h_i , which can be secured from the distribution polygons of figure 6.

Figure 6 furnishes, at the same time, the proof that the difference between acceleration deflection and strain measurements (fig. 1(c)) does not affect the form of distribution. For the appraisals of the He 45, He 70, and Ju 160 were made on acceleration records, while on those for the L 83 and the Ju F 13, the load factor was computed from deflection measurements and for the G 24 from elongation measurements of a beam flange. The plotted frequencies of the first type $h_i = \frac{H_i}{N}$ were computed for

the L 83 and F 13 from counted frequencies of the third type \bar{H}_i , for the others obtained direct by counting. Figure 6 manifests no systematic differences between the results of the individual test methods and types of evaluation.

Subsequently, the distribution polygons were uniformly reduced to the greatest class division $\Delta n = 0.15$ ($n_{\text{safe}} - 1$) shown in figure 6; the results are given in figure 7(a).

This unit distribution is to be, within the widest possible scope, an outside envelope around the measured polygons (fig. 7(a)). That it cannot include the test values outside is due to the fact that the sum $\sum h_i$ of the relative frequencies must be equal to "1" for the unit distribution as well as for everyone of the measured distributions. If all the polygons were fully included, then $\sum h_i > 1$. Since the values h_i decrease very rapidly with increasing values of the absolute amount of $(n - 1)$, the unit distribution for the zones $n > 1$ and $n < 1$ can be so defined that it represents one outside envelope (fig. 7) for all classes except that directly adjacent to the arithmetical mean $\Delta n = 0$. Such a unit distribution is therefore proposed in the treatment of time and fatigue strength problems of wing structures.

The two halves of the polygons for zones $n > 1$ and $n < 1$ are not exactly symmetrical to the arithmetical mean, but rather the distribution is a little fuller for

$n > 1$ than for $n < 1$. (See fig. 7(b).) Now the proof of adequate time or fatigue strength is adduced by fatigue tests in which a static preload, which simulates the stress in unaccelerated horizontal flight ($n = 1$), is superimposed by a periodic additional load through the testing machine. Hereby, it is expedient to choose an oscillating additional loading with equal amplitude upward ($n > 1$) and downward ($n < 1$), and, in order to remain on the safe side, the choice of distribution for the zone $n > 1$ is recommended. As distribution polygon of the periodic additional loads it affords then the solid line of figure 7(b), the ordinates of which are equal to twice the ordinates of the dotted polygons for the zone $n > 1$.

The distribution polygons discussed so far are tied to the chosen class division, that is, an enlargement of the class division effectuates, for example, by constant variation width a reduction in the number of polygon corners and an enlargement of their ordinates. This choice of representation was made purposely as a reminder that the values h_i are not mathematically defined probabilities but experimentally secured relative frequencies, which do not necessarily have to be independent of the experimental object, that is, the individually studied airplane and the scope of the statistics. Because as stipulation for the existence of a mathematical probability representing the limit value of a relative frequency in the event that the scope N of the statistics approaches infinity, there exists the demand that the individual test values either cancel each other, are equally justified and mutually independent or definitely related. Of these only the first condition is satisfied, because the observation of a stress in class i precludes the contemporary measurement of a stress situated in another class. But the test values enjoy equal rights only if the structure of the velocity field of the air over the flight path does not change. This is particularly not the case in flight in ground proximity when ground contour and cover as well as wind velocity and direction are arbitrarily variable along the flight path. Furthermore, Küssner proved the interdependence of the individual stress values in a rigorous examination of the past history, that is, the gusts flown through previously have no effect on the momentarily occurring stress. Since this "previous history" may assume any form, depending upon the accidentally existing local form of the velocity field which changes continuously with respect to time, and which has not the same effect on varying types of

aircraft, there is, at the time, no prospect of adducing proof of the existence of probabilities as limit values of the relative frequencies for the gust stresses of aircraft. Therefore, in the further technical development or by the appearance of new design types, it is necessary to prove anew a unit distribution which appears suitable for an approximate inclusion of all test data.

However, on occasion it may be important to reduce obtained distribution polygons to polygons with a different class division (as in working up specifications or experimental projects). In this instance it is practical to represent the unit distribution in a form independent of the class division. On the other hand, it serves no useful purpose to reduce measured distribution polygons to a lower class division than employed in the evaluation, as instrumental and evaluation errors may then gain considerable influence. Accordingly, only one reduction for the purpose of enlarging the class division is permissible, as a rule.

A form of representation independent of the class division is readily obtainable from a distribution polygon of the frequencies of the second type. The ordinates \bar{h}_i of a distribution polygon of the relative frequencies of the second type indicate the percentage of all measured stress peaks located in the classes, the order of which is greater than or equal to i , that is, what percentage of all stress peaks is greater than or equal to the stress which corresponds to the lower limit of class i . The polygon corners are usually plotted against the center of the class interval as for distribution polygons of the frequencies of the first type. This representation is thus, for the moment, dependent on the class division in the same manner as for the previously discussed frequencies of the first type. But, on plotting the polygon corners against the lower limit of each class interval and connecting the then obtained points by a continuous curve, the latter is, of course, no longer dependent on the class division, since according to definition, the ordinate of each point then indicates the number of load peaks relating to stresses which are greater than or equal to the pertinent abscissa. This curve is termed the summation curve of the distribution, shown in figure 7(c) for the proposed unit distribution (solid line in fig. 7(b)).

It will be noted that the ordinates of the unit distribution polygon deviate so much from one class to the other that the summation curve, after a shift of its points by one-half class width (from class center toward the lower class limit) already is located below the line of the unit distribution. (See figs. 7(b) and 7(c).) In this instance, the summation curve should be used only for converting the distribution polygon to another class division, but not, as customary in other cases, as substitute for the distribution polygon of frequencies of the second kind.

C. Load Reversals for 100 Operating Hours

The prediction of the required time and fatigue strength for a specified total number of hours of operation or of the permissible number of hours of operation for an aircraft wing structure with known time and fatigue strength, stipulates, besides the form of distribution conformable to figure 7, the total number of load reversals within a given time, such as within 100 hours of service, or in other words, the scope N of the total statistics of the stress.

The determination of this value starts with the number of gusts striking the airplane on the average per unit time. This number is largely dependent upon the speed of the aircraft and the degree of gustiness. The effect of longitudinal stability and wing loading may make itself felt on the measured values to the extent that on especially gust susceptible aircraft (low lateral stability, great controlling length = distance wing structure tail, low wing loading) such gusts also produce measurable accelerations, which on less susceptible aircraft merely cause stress fluctuations within the scope of accuracy of the employed instruments. Lastly, the varying damping of the airplane motions may be such that on one aircraft the acceleration due to a gust is aperiodically damped down to lg , while on another there still is a "swing through" to an acceleration value inferior to lg . The effect of these differences on the form of the distribution curves remains, however, within the usual spread bands. (Cf. fig. 6.)

In figure 8 is shown for two He 45 type of aircraft the mean gust frequency ν recorded in a series of test flights at an average speed $v = 270$ km/h, that is, the

total number of upgusts and downgusts per second plotted against the Darmstadt gust scale (dashed lines in fig. 8(a)); the two airplanes had the same gross weight but different center of pressure positions. The recorded gust frequencies are seen to average a little higher on the less longitudinally stable aircraft than on the other. The same holds true for figure 8(b), where, next to the values for the two He 45 types, the gust frequency on an He 70 type at the same speed is plotted against the degree of gust; the He 70 has less static longitudinal stability than the He 45. The maximum discrepancies occur, as expected, in the low-gust range.

In averaging over a longer operating period the mean gust frequencies secured for the individual gust degrees must, in conformity with the average yearly probability of appearance of the individual gustiness degrees, be provided with "weights." Observations of the frequency of appearance of gusts of various degrees are cited in the next chapter. Using the yearly averages given there for the Adlershof airport as basis, the yearly averages for the He 45 are those shown in figure 8(a). The yearly average of the He 70 is indicated in figure 8(b). These averages refer to a 270 km/h flying speed.

The extent to which the gust frequency depends upon the flying speed is illustrated for the He 70 in figure 9. All plotted test values for the He 70 refer to flights with the same weight and the same center of pressure position. Averaging straight lines drawn through the test points of equal gustiness pass through the origin of the coordinate system. Further averages formed between these individual straight lines by the use of "weights" conformable to the probability of appearance of the particular gust intensity, give as yearly average for the He 70 the relation of gust frequency to flying speed shown by the solid line. For the He 45 the only known point is that for a 270 km/h flying speed according to figure 8(a). Presuming that the relationship between gust frequency and flying speed can be represented for the He 45 also by a straight line through the origin of the coordinates results in the He 45 line as shown in figure 9. The gust frequencies recorded so far on other types of aircraft range between these two straight lines.

In a deduction of the load reversal expectancy for a given operating period from the gust frequencies v of figures 8 and 9 with the help of figure 7, it is to be

noted that the gust frequency ν indicates the number of upgusts and downgusts per unit of time. But since one load cycle defines an upgust and a downgust of equal intensity, the total number of load reversals expected in time interval $T(s)$ is:

$$N = \frac{\nu}{2} T$$

In as much as modern airplanes of stress category 3 will undoubtedly be similar to the type He 70 as far as flight characteristics are concerned, the solid line of figure 9 may be used as a basis in the calculation of the load reversal expectancy, that is,

$$\frac{\nu}{2} \approx 0.0115 \nu \text{ (1/s), } (\nu \text{ in m/s})$$

which amounts to $N \approx 4100 \nu$ load reversals for 100 hours of operation. This data in conjunction with figure 7 serves for the time being as the required time and fatigue strength for wing structures of aircraft of stress category 3.

Since the data on gust frequencies are obtained by evaluation from acceleration records, they naturally do not contain the wing oscillations shown superimposed in figure 1c, as the reaction of these oscillations on the fuselage creates no measurable accelerations. On the Albatros L 83 and the Ju F 13 the actual count disclosed that allowance for these minor cumulative oscillations raises the frequencies about threefold. Even so it does not appear justifiable to include this effect in the determination of the required load reversals, since the small cumulative oscillations are not likely to be decisive for the fatigue strength,* and the unit distribution as well as the determination of ν was secured on the basis of the upper limit of the past range of experience. In this respect it further should be remembered that all flight

*F. Bollenrath has pointed out that these cumulative oscillations with small amplitude might possibly increase the fatigue strength of a component; their omission therefore is perhaps an added safety.

measurements are made in the particularly turbulent air layers near the ground, so that in reality lower operating stresses occur in all the airplanes which, throughout a substantial period of life, are encountered at heights above 1000 meters.

Additional free flight measurements with special regard to the effect of flying speed, static longitudinal stability, and controlling length on the gust stresses will serve to perfect the necessary data on gust frequencies.

D. Gustiness in the Atmosphere

(by the Darmstadt Gust Scale)

For the comparison of different test flights from stress measurements in gusty weather, some indication for the gustiness on the day of the test is imperative. For a more accurate description of the gustiness it would require special frequency studies of the controlling meteorological values, as, for example, momentary horizontal wind velocity at flying altitude and velocity in vertical gusts. Such an investigation is, however, difficult, and the evaluation of the measurements more time consuming than that of the stress measurement itself. For which reason investigations of this kind are provided for independently from the test flights at the Lindenberg Aeronautic Observatory, where, in collaboration with the DVL, measurements are to be made on the structure of the velocity field in gusty weather and on the order of magnitude of the gradients of the velocity field, the data of which are to serve as basis for systematic calculations of gust stresses, and particularly, regarding the effect of the static longitudinal stability and the controlling length.

A simpler description of the gustiness at the day of the test being necessary for the present analysis, an attempt was made to use the Darmstadt gust scale (reference 4) employed at the weather stations. This scale is graduated as follows:

DARMSTÄDT GUST SCALE

Applicable to Junkers A 20 and Similar Types

Scale division	Characteristics	Symptoms
$b_0 = \text{gust } 0$	slight unrest	Airplane balances easily or individual slight bumps. No rudder action to equalize bumps - engine rpm constant - dynamic pressure constant.
$b_1 = \text{gust } 1$	moderate unrest	Airplane oscillates frequently about fuselage axis - moderate rolling motions - repeated slight aileron operation necessary - rpm constant - occasional dynamic pressure fluctuations.
$b_2 = \text{gust } 2$	strong unrest	Airplane leaves course - rolls (dances) - continuous operation of rudder and ailerons necessary - crew feels being raised from and pushed down in seat - feeling as in an elevator - engine audibly picks up, perceptible fluctuations of rpm and of dynamic pressure.
$b_3 = \text{gust } 3$	severe unrest	Airplane pancakes or zooms - sideslips repeatedly - response to control deflection heavy - crew is raised from seats (hang from straps) - strong pickup of engine (alternating howling noises), marked change in rpm and dynamic pressure.

All the pilots of the DVL making test flights at the Adlershof airport, therefore, were requested to give a report of the gustiness for every flight according to the Darmstadt scale. The statistics collected so far cover 24 months. These were supplemented by the statistics collected at seven weather stations. The two sets of statistics are compared for the purpose of checking the applicability of the Darmstadt gust scale to the problem in question. Table IIIa gives the average values of the probable appearance of the individual gust intensities according to the DVL statistics for July to December 1935 and 1936, while table IIIb gives the averages for two years according to the DVL statistics in comparison with the averages from the seven governmental weather stations. Figure 10 shows various distributions. All data refer to 0 to 1000 meters altitude range; at greater heights the gustiness is less on the average.

TABLE IIIa

Gust degree	July		August		September		October		November		December	
	1935	1936	1935	1936	1935	1936	1935	1936	1935	1936	1935	1936
quiet	2.4	0	5	1.6	7.4	2.9	11.1	0	4	0	0	0
b ₀	35.1	45.4	43.7	33.3	41.7	47.8	55.0	45	80	64.1	53.5	77.5
b ₁	44.6	51.5	44.6	52.4	33.3	44.9	26.7	42.6	16	32.8	44.2	18.4
b ₂	13.1	3.1	6.7	11.1	13	4.4	7.2	10.9	0	3.1	2.3	4.1
b ₃	4.8	0	0	1.6	4.6	0	0	1.5	0	0	0	0

TABLE IIIb

Gust degree	DVL		DVL	Weather stations	
	July 1935 to June 1936	July 1936 to June 1937	July 1935 to June 1937	January to December 1935	January to December 1936
quiet	3.2	0.6	1.9	69.5	72.8
b ₀	48	57.7	52.9	6.5	5.4
b ₁	38.9	35.8	37.3	16.1	15.1
b ₂	8.9	5.6	7.3	7.4	6.2
b ₃	1	.3	.6	.5	.5

A close agreement obtains between the statistics from both sources respecting the probable appearance of greater gustiness (2° and 3°), while substantial discrepancies exist between "still" to " b_1 ," for instance, the report "still" in the DVL statistics appears in barely 3 percent of the cases, while in about 70 percent of the cases the observers at the weather stations did not think it worthwhile to report. As a result, the DVL pilots reported a greater number of gust occurrences of the order of b_0 or b_1 than the weather stations. The reason for this discrepancy might be due to the fact that a number of the fine measurements in the DVL can be effected only in perfectly still air, so that flights in very slight gusts had to be stopped. In all these cases gust reports were naturally turned in, while meteorologically such slight gusts are in most cases unnoticeable and utterly inessential for flight safety, hence were not reported by the weather stations. Aside from this a certain amount of scattering naturally was to be expected since the flights were made at different localities with dissimilar types of aircraft and by different pilots so that even within the same group of observers a certain amount of scattering was noticeable. But no great systematic discrepancies between different airplane types have been found by the DVL, so that a division in this respect did not appear necessary. Theoretically the data according to the Darmstadt gust scale for a simple description of gustiness are practical, especially if the collection of the gust statistics and the execution of the test flights remain in the same hand.

The averaging of the previous gust frequencies (fig. 8) was made on the basis of the average values of the DVL statistics for the period of July 1, 1935 to June 30, 1936.

IV DISTRIBUTION CURVES OF THE OPERATING STRESSES

IN ACROBATIC WING STRUCTURES

While on airplanes of stress categories 2 and 3 intended for air line service, the stresses due to pilot control actuation generally play no decisive part in time and fatigue strength studies and are included in the operating stress measurements, the stresses in acrobatic aircraft, induced by the pilot must be studied separately.

In this respect the little available data concerns three acrobatic types of aircraft, as compiled from the recorded number of acrobatic evolutions shown in figure 11. These flights were made by a number of licensed stunt pilots with more or less practice. This applies particularly to the measurements on the He 51 type. The following evolutions were flown:

1. He 46 (approved for acrobatic flight 1 only)
 - loop
 - wing-over
 - renversement (half loop and half roll)
2. FW 44 (all acrobatics)
 - with observer:
 - loop
 - wing-over
 - snap roll
 - Immelmann turn
 - renversement
 - steep turns
 - without observer:
 - elevator operation in inverted flight
 - outside loop starting from inverted flight
 - and from normal flight
3. He 51 (all acrobatics)
 - loops
 - wing-over
 - snap roll
 - renversement

In spite of the comparative scarcity of test data, an average distribution is afforded (solid line, fig. 11) which holds for these three types, even though the scattering is bound to be greater than for the far more elaborate gust stress statistics in chapter III. The permissible lower limits of the safe load factor n_{safe} for aircraft of stress categories 4 (acrobatics 1) and 5 (acrobatics 2) are given in figure 11. The values served as basis for the three explored types and are in the following used as reference data for the recorded stresses.

Figure 12 shows the average distribution curve of figure 11, the values being given in fractions of $n_{safe} - 1$ for category 4. Instead of the relative frequencies, the load reversal expectancy in 100 hours of operation is

plotted as ordinate, proceeding from 75 load reversals in 1 hour (used in acrobatic flight training).

Aside from the stresses in stunt flying, acrobatic airplanes naturally are subject to gust stresses the height of which the pilot cannot or can only slightly control. Assuming an acrobatic airplane of stress category 4 is never used throughout its life for acrobatics but exclusively in distance operation, the gust stress distribution curve differs from that given in figure 7 for category 3 to the extent that the gust load factor $n_{G_{safe}}$ (range 1.15 of the BVF, edition 1935) is considerably below the safe load factor for category 4. For the usual airplane types it is about

$$\frac{2}{3} (n_{safe} - 1) \leq n_{G_{safe}} - 1 \leq \frac{5}{6} (n_{safe} - 1)$$

The gust stress distribution curve for the upper limit $\frac{5}{6} (n_{safe} - 1)$ is shown as thin line in figure 12. The load reversals for 100 hours of operation are computed with $\frac{N}{2} = 1/s$.

It is, of course, impossible to predict the extent to which an acrobatic airplane will be used during its lifetime for acrobatics in calm weather and for ordinary travel in gusty weather. But it is found that the requirements will not be too severe if the worst possible assumption is made that the acrobatic flight stresses are simply superimposed on the gust stresses. The then resultant distribution (heavy curve in fig. 12) touches in the range of high load reversals, that is, under stresses within the range of alternating strength, the distribution for gust stresses, and touches, by safe load, the distribution curve for acrobatic flight stresses. Appreciable differences occur only under stresses of the order of magnitude of $0.5 (n_{safe} - 1)$. If, for stresses of this magnitude, the compliance with the strength requirement (illustrated by solid curve in fig. 12) should cause structural difficulties, some moderation could be made in this region.

V. TEMPORARY RULES GOVERNING THE REQUIRED STRENGTH
OF AIRCRAFT WING STRUCTURES UNDER FREQUENTLY
RECURRING STRESSES.

Cipher 1015 of the "Strength Specifications for Aircraft, edition December 1936" reads as follows:

1015: At $j = 1.35$,* that is, by concurrent increase of the static load proportion and the superimposed alternating load each to 1.35 times their amount, precisely those stress limits may be reached which, if exceeded by the load reversal expectancy during the total operating period of the aircraft, would result in fatigue failure of the particular part.

This specification requires an amendment stating what load reversals are to be conjugated to certain amounts of the alternating load if the total operating period during the lifetime of an airplane part is prescribed as required value.

With the foregoing data certain rules governing the strength specifications of wing structures under repeated stresses can be put forth. As "static load proportion" the load on the relevant part in stationary horizontal flight (load factor $n = 1$) is chosen.

As alternating stresses to be superimposed on the static load portion, the distribution polygons of the load reversals belonging to certain values of the alternating stress can be secured from figures 7 and 9, 11 and 12, respectively. This leaves one on the safe side since some differences exist between the type of stress in actual flight and in a static test. First, in a test it is practically impossible to simulate the stresses corresponding to the individual gusts or flight figures in

* j = safety factor; the high value 1.35 came into being at a time when the type of "strength tests under repeated stress in the sense of flight statistics" recommended here, (definition according to Teichmann and Gassner, who originally started a systematic study of such tests at the time in the DVL) had not yet been taken into consideration.

somewhat the same way; the practice is to let continuously smaller groups of identical loads follow successively. But there are very few experiences on what effect this discrepancy between stress sequence in flight and that of the component in a fatigue test will have. On the other hand, there are usually no pauses in fatigue tests such as occur between flights. So the extent of the effects of such intervals on the strength under repeated stress in the favorable sense remain unknown at the present stage. Lastly, to shorten the time in testing, the loads are often applied at much greater frequency than corresponds to the mean load frequency in flight operation. In the absence of sufficient research data on the combined effects of these three factors, the specifications on which the tests are made must be formulated with care, since the safety factor j is primarily intended to cover the experimental scattering.

For this reason the distribution polygon of the load reversals due to gust stresses has been based upon the unit distribution of figure 7 which comprises nearly all the test values of the relative frequencies. As gust frequencies the maximum values of figure 9 (solid line) are chosen, which represents the upper limit of the empirical range for the case that the flight of an airplane throughout its lifetime is exclusively below 600 meters, where severe gustiness is most frequently encountered. The acrobatic flight stresses base on figures 11 and 12 on the assumption that the particular airplane is continuously used for acrobatic flight training.

The corresponding distribution polygons for stress categories 2 and 3 and 4, respectively, and the related summation curves are given in figures 13 and 14, the pertinent distribution tables in tables IV and V. The previously described assumptions on which these tables and charts are based, should insure that the required time and fatigue strength is sufficient to also cover the previously described uncertainties.

TABLE IV
DISTRIBUTION TABLES FOR FIGURE 13

Fraction of ($n_{\text{safe}} - 1$)	$H \times 10^{-3}$ for categories 2 and 3	$H \times 10^{-3}$ category 4
0.075	281	315
.225	65.7	44
.375	11.5	6.35
.525	1.44	1.44
.675	.432	.578
.825	.131	.334
.975	.050	.190
1.125	.016	.127

TABLE V
ORDINATES FOR FIGURE 14

Fraction of ($n_{\text{safe}} - 1$)	$\Sigma H \times 10^{-3}$ categories 2 and 3	$\Sigma H \times 10^{-3}$ category 4
0	360	370
.15	79	53
.30	13.6	9.02
.45	2.07	2.67
.60	.629	1.23
.75	.197	.651
.90	.066	.317
1.05	.016	.127

The quoted load reversals are calculated for a value of $\frac{1}{2}$ gust frequency $\frac{v}{2} = 1/s$. It is obtained at a flying speed of $v_h \approx 90 \text{ m/s} \approx 350 \text{ km/h}$. For airplanes with higher top speeds v_h in stress category 3, all posted load reversals in stress category 4, the load reversals defined by the gust stresses, that is, the reversals for stress values $0.1(n_{\text{safe}} - 1)$ up to about $0.5(n_{\text{safe}} - 1)$ must be raised in the ratio $\frac{v_h}{90}$ (v_h in m/s).

To secure from figure 13 the load reversals required for wing structures in the individual load stages, the figures given there must be multiplied by the required or desired (by the purchaser) total operating hours of an airplane (in the unit of 100 hours of operation). It should average about 6000 hours for commercial and about 2000 hours for acrobatic types. In the static test the total number of loads to be applied are suitably divided in groups of several hundred hours each; these groups, each of which comprises individually all load stages, are successively applied to the structural part in question. The required load reversals for category 5 range between the values of categories 3 and 4. So long as no adequate data on acrobatic flight stresses are available, the load reversals specified for category 4 are recommended for those of category 5 also.

Analyzing the order of magnitude of load reversals throughout the total operating hours in question, it is seen that in the lowest load stage only load reversals of several millions are encountered, which suggests a comparison of this load stage with the pure fatigue strength of the design. But this is inadmissible for two reasons: First, the effect of the loads appearing in the higher load stages would be completely ignored; second, according to the available strength tests it is likely to be much more difficult on the conventional wing structure designs to comply with the requirements in the higher load stages, that is, in the region of the time strength. Available experiences on fatigue strength of structural components are therefore unsuitable for estimation of the safety of a wing structure in protracted flight operation, it is always necessary to make suitable load tests in the sense of flight statistics.

Translation by J. Vanier,
National Advisory Committee
for Aeronautics.

REFERENCES

1. Preisausschreiben für einen Wettbewerb um einen aufzeichnenden Beschleunigungsmesser für Flugzeuge. Jahrbuch 1913-14 der Wissenschaftlichen Gesellschaft für Flugtechnik, Berlin 1941, pp. 31-34.
2. Küssner, H. G.: Stresses Produced in Airplane Wings by Gusts. T.M. No. 654, NACA, 1932.
3. Küssner, H. G.: Häufigkeitsbetrachtungen zur Ermittlung der erforderlichen Festigkeit von Flugzeugen. Luftf.-Forsch., Bd. 12, Lfg. 2, May 16, 1935, pp. 57-61.
4. Lange, K. O.: Die Darmstädter Böigkeitsskala. Beiträge zur Physik der freien Atmosphäre, Bd. 17, 1931, pp. 89-101.
5. Fechner, G. Th.: Kollektivmasslehre. (Leipzig). 1897.
6. Bruns, H. Wahrscheinlichkeitsrechnung und Kollektivmasslehre. (Leipzig), 1906.
7. Czuber, E.: Die statistischen Forschungsmethoden. (Wien), 1927.
8. Rietz, H. L.: Handbuch der mathematischen Statistik (deutsche Ausgabe von F. Baur). (Leipzig und Berlin), 1930.
9. Bauvorschriften für Flugzeuge, Heft 1: Vorschriften für die Festigkeit von Flugzeugen, Neudruck Fassung, December 1936.

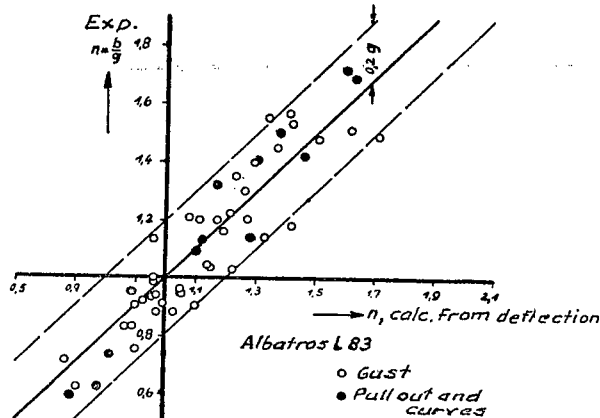


Figure 1a.-Load factors, experimental and as computed from wing deflections.

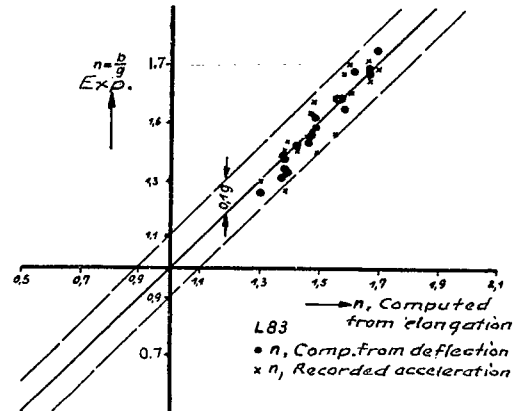


Figure 1b.-Load factors, experimental and as computed from the strains of a beam flange (the relative values computed from the wing deflection are included).

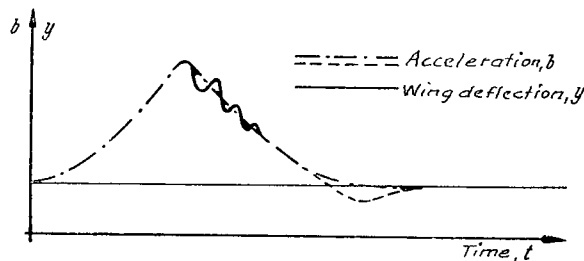


Figure 1c.-Wing deflection and acceleration during a gust.

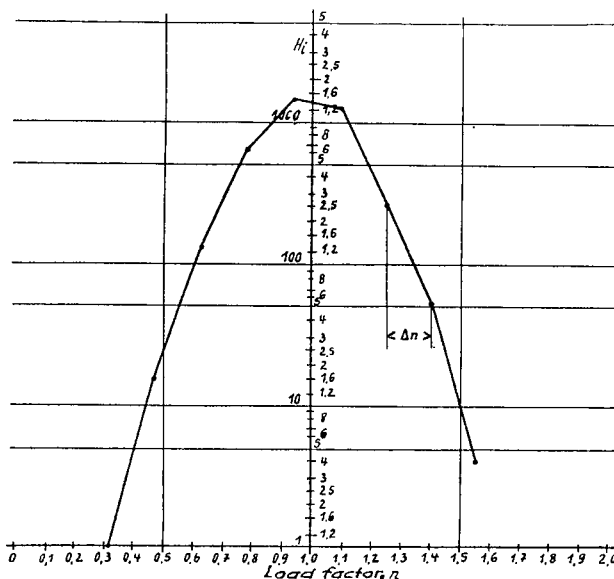


Figure 2.-Distribution polygon for Table 1. The counted frequencies H_i are conjugate to the middle of the class interval used in the count, as argument value Y_i .

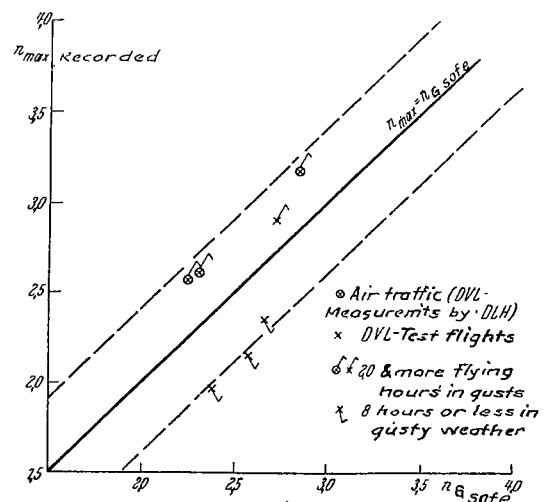


Figure 3.-Maximum load factor n_{\max} recorded in flights in gusty weather compared with the value n_g safe for $v=v$ cruising on seven different type aircraft.

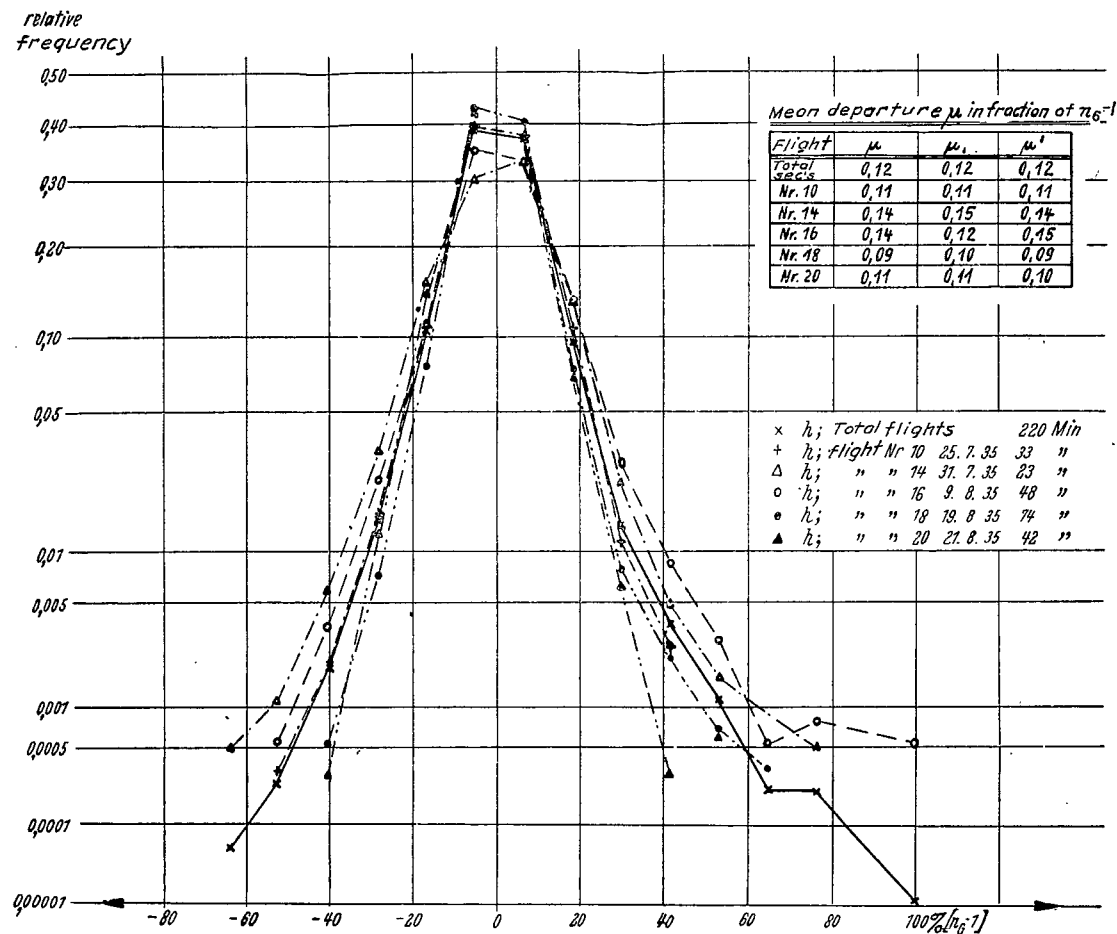


Figure 4.-Distribution polygons for 5 different flights with He 45 D, D-JDUH, at gust scale b_1 . gust load factor $n_G=2.71$.

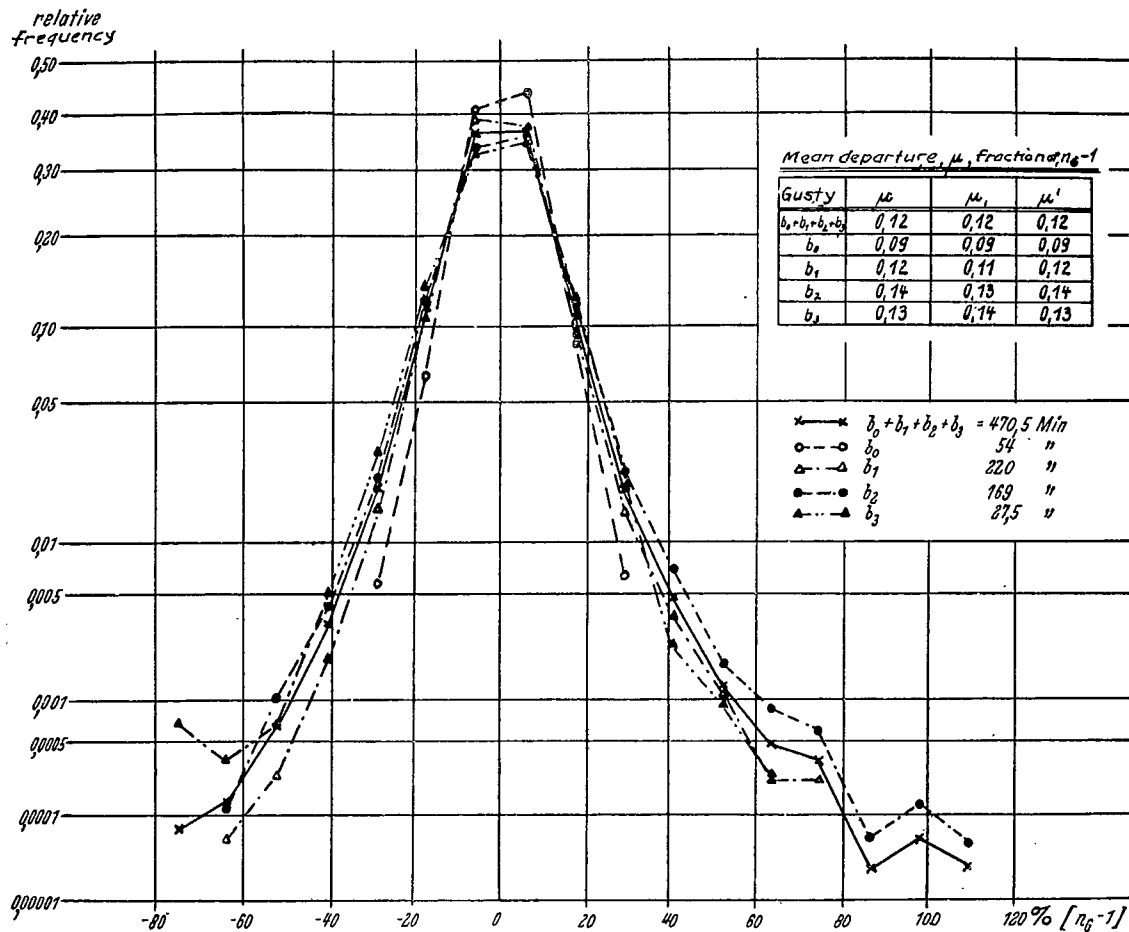


Figure 5.-Distribution polygons for 5 different flights with He 45 D, D-JDUM, at gust scale b_0 , b_1 , b_2 , b_3 . gust load factor $n_G = 2.71$.

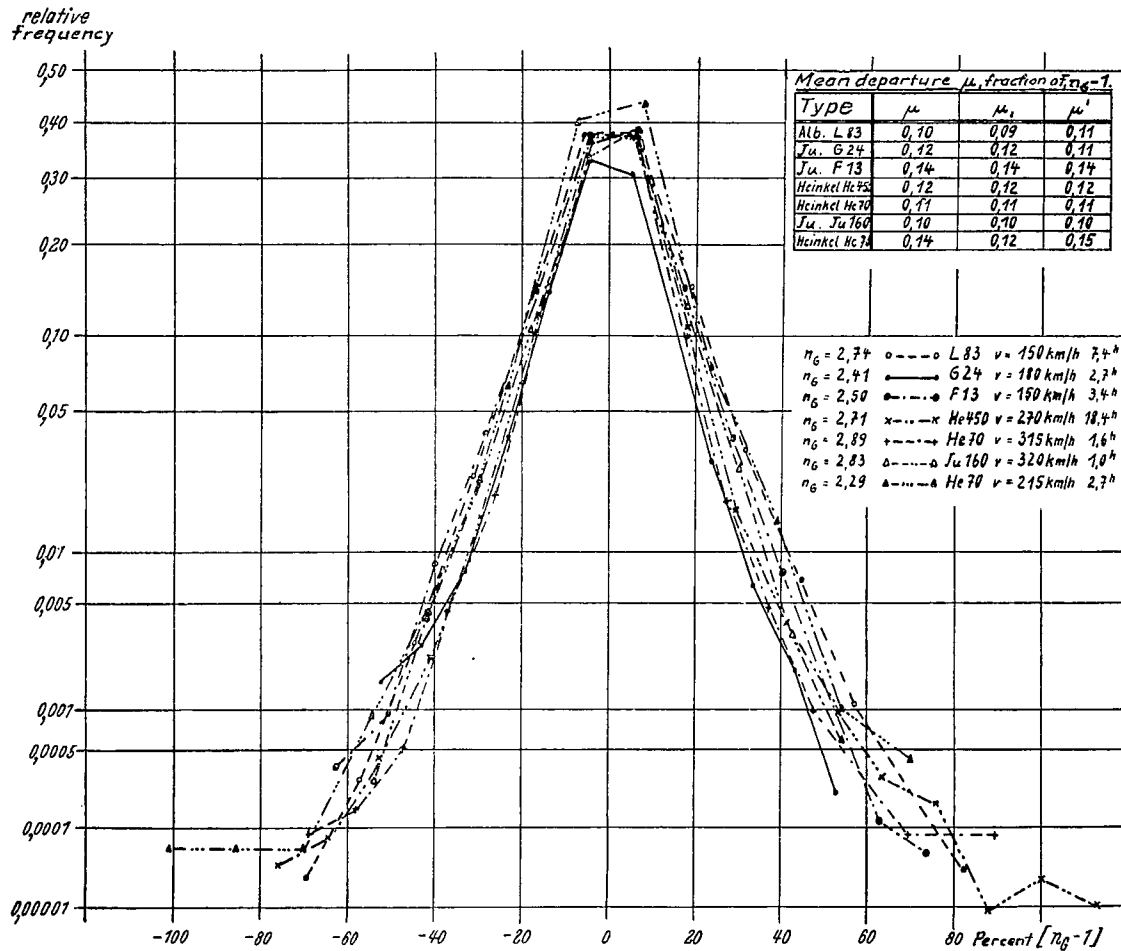


Figure 6.- Distribution polygons for 6 different types of aircraft.

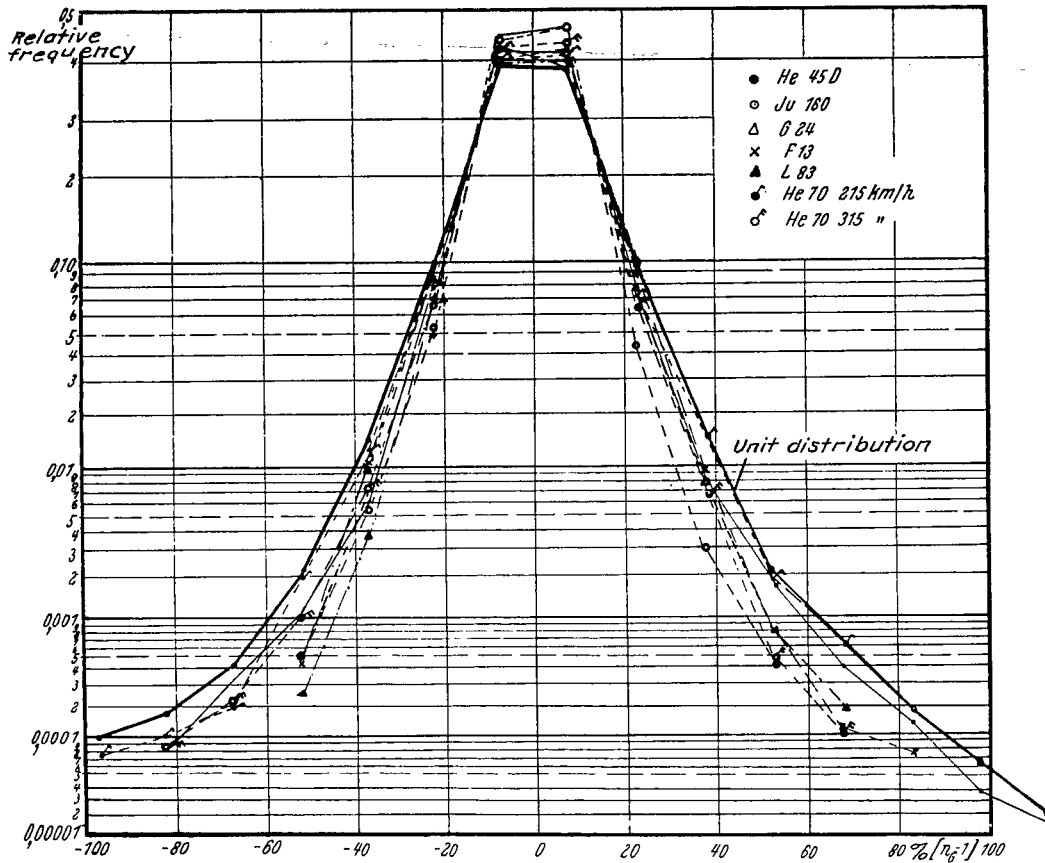


Figure 7a.-Distribution polygons of Figure 6, reduced to class division $\Delta n = 0.15(n_c - 1)$.

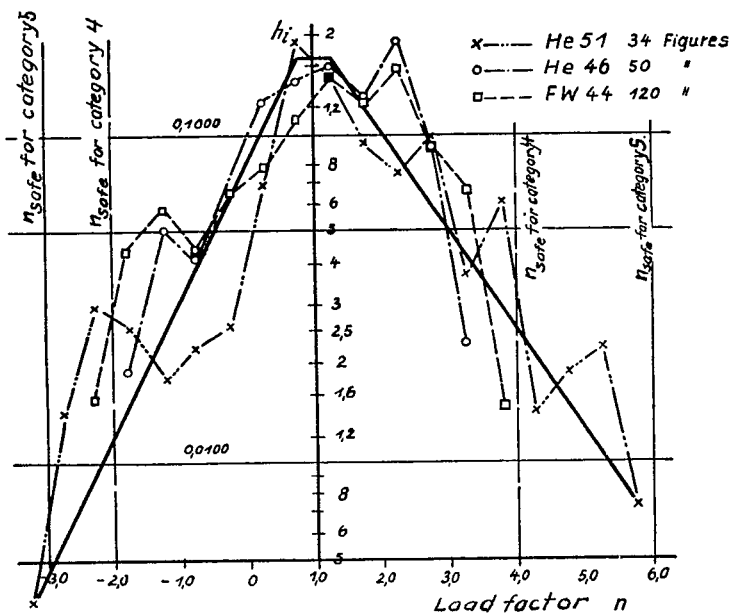


Figure 11.-Distribution polygons of acrobatic flight stresses for 3 types of aircraft.

Figure 7b.-
Unit
distribution
for zones
 $n > 1$ and
 $n < 1$.

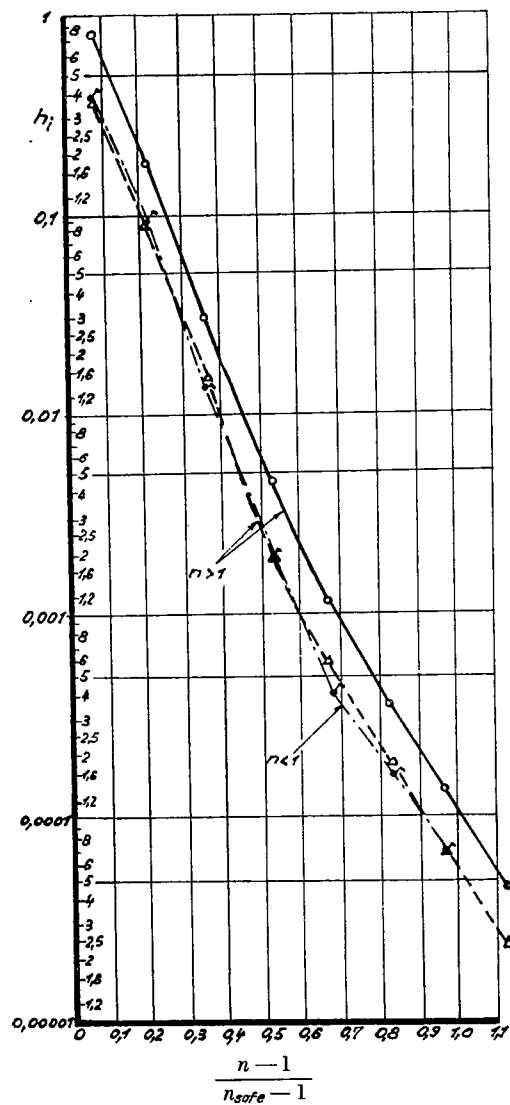
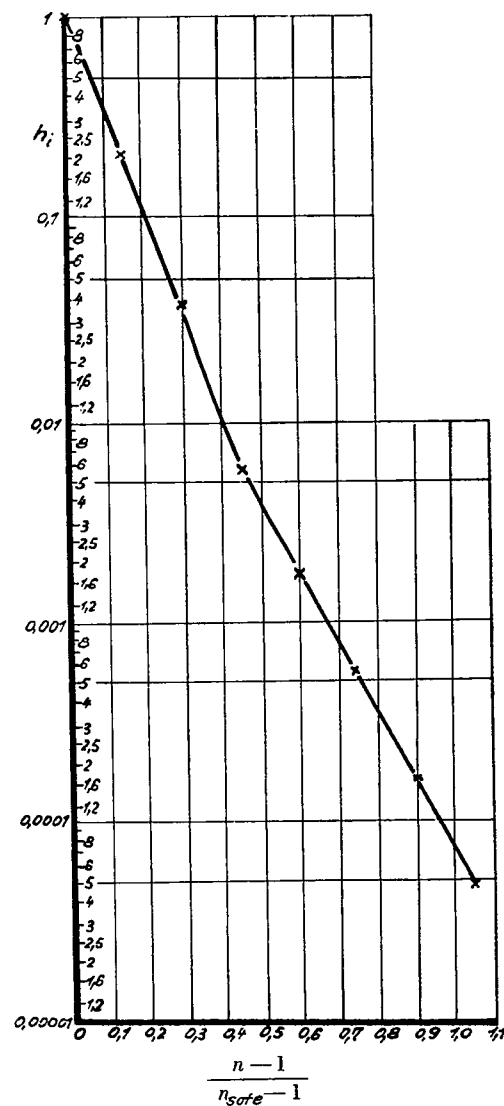


Figure 7c.-
Summation
curve of
unit
distribution.



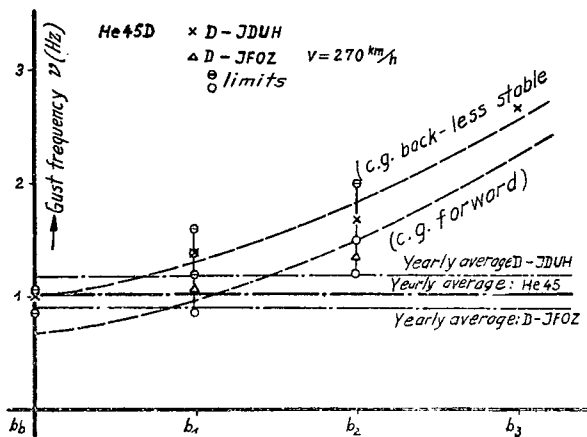


Figure 8a.-Gust frequency for two H 45 at different c.g. position in relation to gustiness.

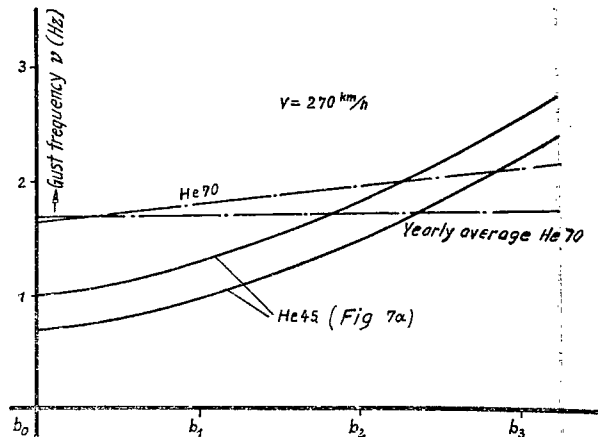


Figure 8b.-Gust frequency for two H 45 at different c.g. position in relation to gustiness.

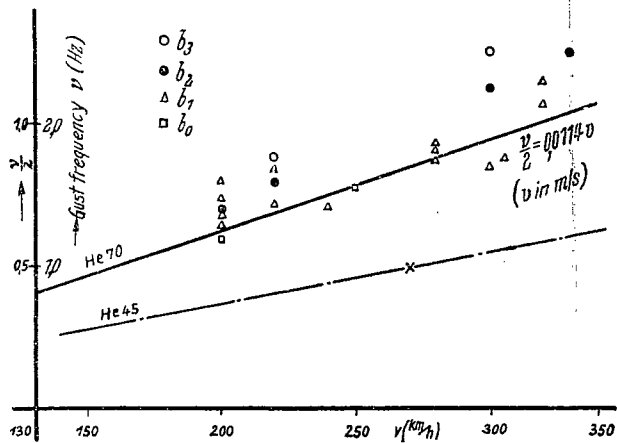


Figure 9.- Gust frequency against flying speed.

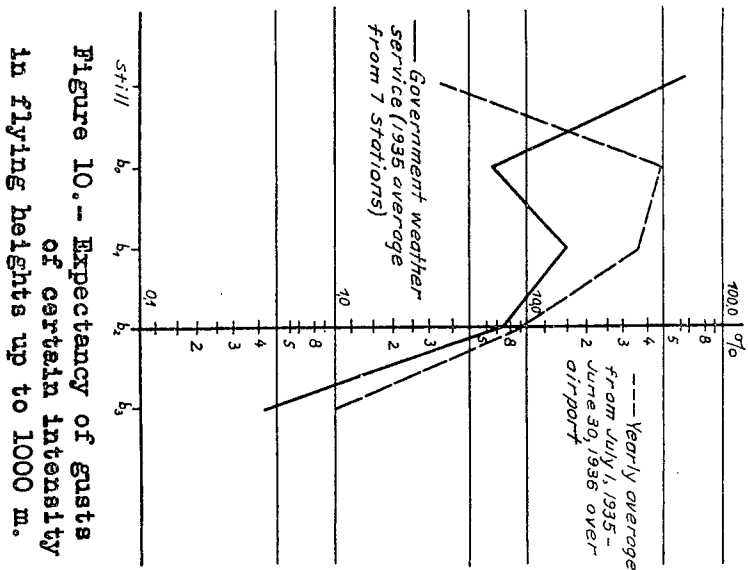


Figure 10.- Expectancy of gusts of certain intensity in flying heights up to 1000 m.

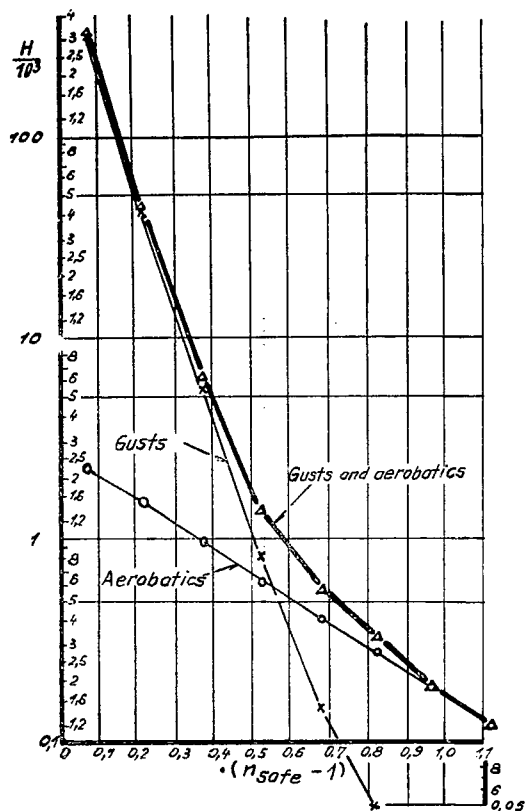


Figure 12.-Load reversals H for 100 hours of operation in acrobatic aircraft of stress group 4.

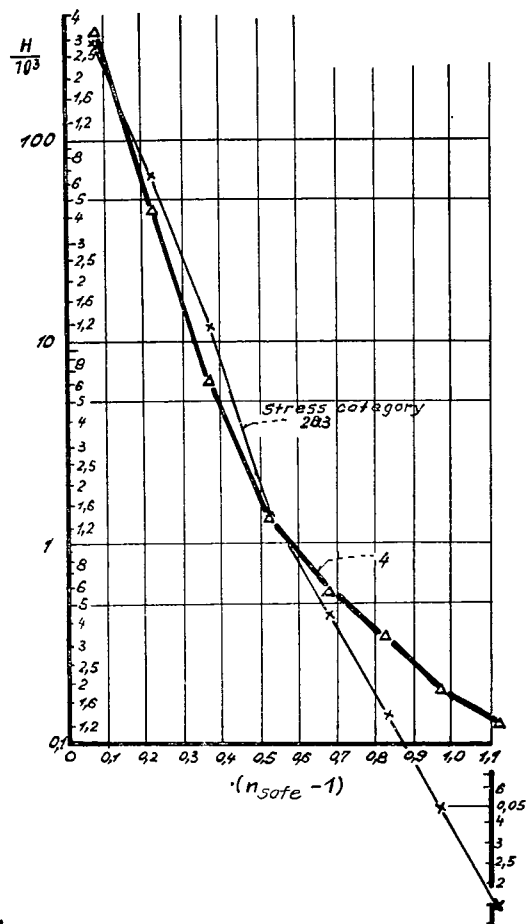


Figure 13.-Load reversals H for 100 hours of operation in aircraft of stress groups 2, 3, and 4.

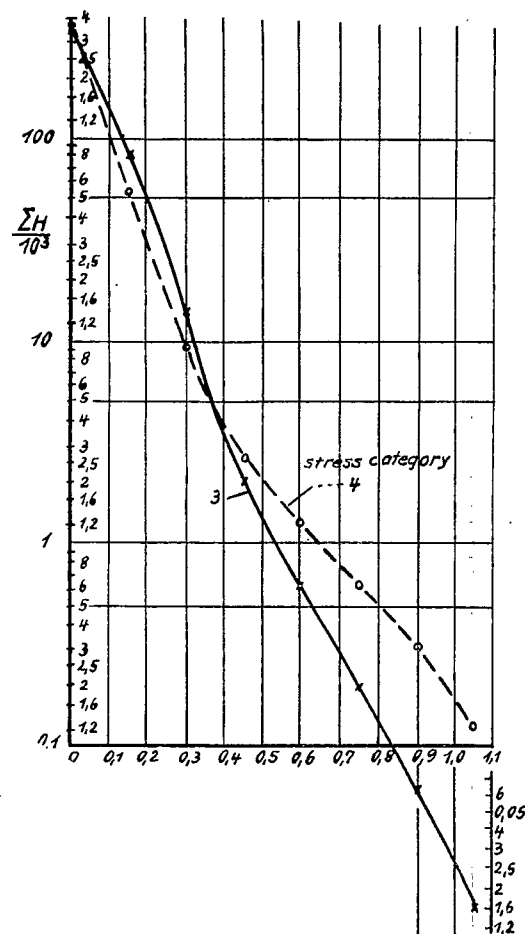


Figure 14.-Summation curve for figure 13.

NASA Technical Library



3 1176 01440 4116